Project Description

September 10, 2004

1 Introduction

1.1 Status of Neutrino Oscillations and Next Steps

1.2 Reactor experiment: Contributions and comparisons

For a three active neutrino scenario, neutrino oscillations are described by six physics parameters: $\theta_{13}, \theta_{12}, \theta_{23}, \Delta m^2_{12}, \Delta m^2_{23}$, and the CP violation phase, δ. In addition, a full description also requires knowing the hierarchy of mass state 3 relative to 1 and 2, *i.e.* the sign of Δm^2_{23}. Of the six parameters, $\theta_{12}, \sin^2 2\theta_{23}, \Delta m^2_{12}$, and Δm^2_{23} are fairly well known and will be addressed with greater precision through the current and planned long-baseline programs (SuperK, Minos, T2K, Nova and CNGS). This leaves for determination θ_{13}, δ, the value of θ_{23}, and the mass hierarchy. Reactor measurements directly address contraints on θ_{13} and θ_{23} which provides extra ingredients that needed to move towards determining δ and mass hierarchy.

The leading order dependence of the oscillation probability for reactor and long-baseline measurements is given by

$$P_{reactor} = 1 - P(\nu_e \to \nu_e) \simeq \sin^2 2\theta_{13} \sin^2 \left(1.27 \Delta m^2_{31} L/E\right) + \cdots$$

$$\begin{aligned} P_{long-baseline} &= P(\nu_\mu \to \nu_e) \simeq \sin^2 2\theta_{13} \sin^2 \theta_{23} \sin^2 \left(1.27 \Delta m^2_{31} L/E\right) + \\ &+ \text{ Other terms with CP viol. and matter effects} \end{aligned}$$

The higher order corrections for the reactor probability are quite small for the Braidwood experimental layout and so a measurement of $P_{reactor}$ directly constrains the mixing parameter θ_{13}. On the other hand, the full expression for the long-baseline probability introduces many degeneracies and correlations between the physics parameters θ_{23} and δ_{CP}, plus the mass hierarchy through matter effects even before experimental uncertainties are taken into account [?, ?]. Therefore, a measurement of $P_{long-baseline}$ corresponds to sizeable regions in the physics parameter space. For this reason, a reactor experiment is ideal for determining θ_{13} and, in combination with the offaxis data,constraining θ_{23}.

As will be shown in the following sections, the Braidwood experiment will have a sensitivity equal or better than $\sin^2 2\theta_{13} = 0.01$ at the 90% CL. For most of parameter space, this is better in constraining the true value of $\sin^2 2\theta_{13}$ than either the T2K or Nova experiments even with the intensity upgrades being proposed as shown in Figure 1. The size of θ_{13} sets the scale for which the off-axis experiments can start to probe CP violation and the mass hieracrchy. A combination of T2K and Nova will start to give some information about these effects if $\sin^2 2\theta_{13} > 0.05$ and, as shown in Figure 2, with enhanced beam rates will have good coverage if $\sin^2 2\theta_{13} > 0.03$ level. Thus, an unambiguous determination of $\sin^2 2\theta_{13}$ at the 0.01 level from a reactor experiment is a crucial ingredient in planning the strategy for an oscillation program, as well as accessing the phenomenology of neutrino mixing.

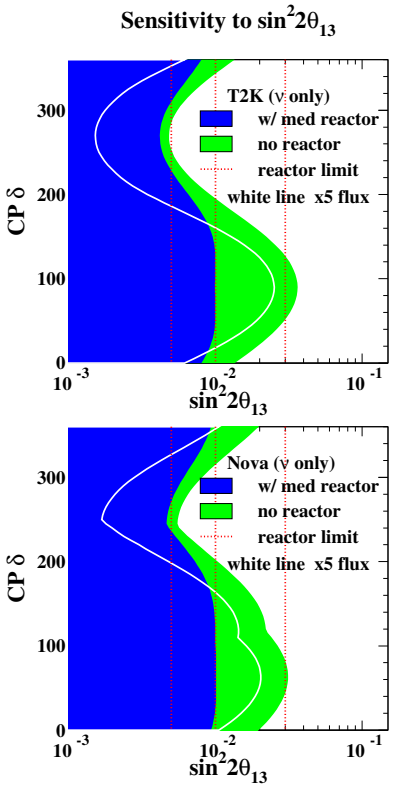

Figure 1: 90% C.L. upper limit regions for various oscillation measurements for an underlying null oscillation scenario where $\sin^2 2\theta_{13} = 0$ ($\sin^2 2\theta_{23} = 0.95 \pm 0.01$, $\Delta m^2 = 2.5 \pm 0.01 \times 10^{-3}$ eV^2 and $\delta_{CP} = 0^0$). The left (right) plot is for the T2K (Nova) long-baseline experiment. The vertical dotted line in each plot correspond to the 90% C.L. upper limit from a Braidwood reactor measurement. The grey region (white curve) is the 90% C.L. allowed region for the long-baseline experiments for a three year neutrino only run with nominal ($\times 5$) beam rate and the black region gives the combination with the Braidwood measurement.

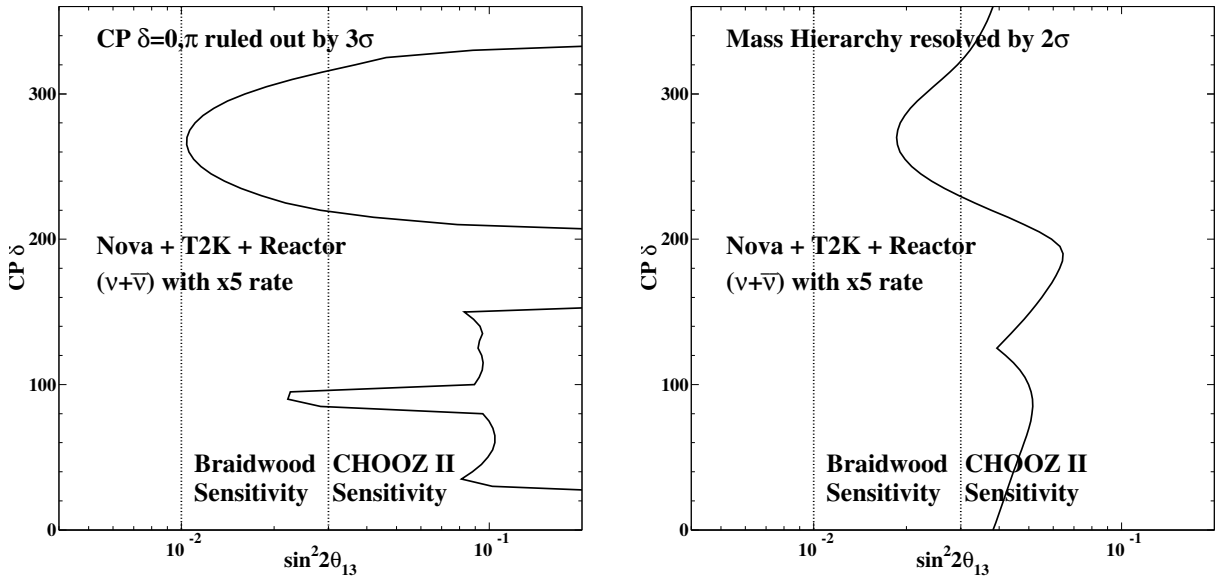

Figure 2: Regions of true CP phase δ versus true $\sin^2 2\theta_{13}$ where: (Left) a combination of data can observe CP violation at the three standard deviation level and (Right) the combination of data can resolve the mass hierarchy at the two standard deviation level. The assumed data is a combination the T2K, Noνa and a Braidwood type reactor experiments. For both plots, the T2K and Nova data sets are assumed to be with upgraded beam fluxes ($\times 5$ the nominal rate) as would be expected with new proton drivers. The two vertical lines in both plots represent the 90% C.L. $\sin^2 2\theta_{13}$ sensitivities for the CHOOZ II and Braidwood type reactor experiments.

1.3 Elastic Scattering Measurements at Reactor Experiments

The availability of a high statistics, high precision reactor neutrino experiment provides an ideal environment to search for new exotic physics. In particular, one can use neutrino-electron scattering to make precision tests of what is predicted by the Standard Model. Neutrino-electron scattering is sensitive to one of the most fundamental parameters in the Standard Model of particle interactions, the weak mixing angle. Deviations from theoretical prediction would be evidence of new physics processes at work.

The differential cross-section for $\bar{\nu}_e + e^- \rightarrow \bar{\nu}_e + e^-$ scattering is given by the following expression [1]:

$$\frac{d\sigma}{dT} = \frac{G_F^2 m_e}{2\pi}[(g_V + g_A)^2 + (g_V - g_A)^2(1 - \frac{T}{E_\nu})^2 + (g_A^2 - g_V^2)\frac{m_e T}{E_\nu^2}] + \frac{\pi\alpha^2\mu_\nu^2}{m_e^2}\frac{(1 - T/E_\nu)}{T} \quad (1)$$

where E_ν is the incident $\bar{\nu}_e$ energy, T is the electron recoil kinetic energy, and the vector and axial vector coupling constants are given by:

$$g_V = 2\sin^2\theta_W + \frac{1}{2} \qquad g_A = -\frac{1}{2} \quad (2)$$

The electron scattering cross-section allows a direct measurement of the weak mixing angle θ_W. As such a process is purely leptonic, it is void of uncertainties associated with nuclear structure or strong interactions. A high precision future measurement of the weak mixing angle is motivated, in part, by the result report by the NuTeV experiment, who measures a 3σ deviation from Standard Model predictions [2]. Various exotic models to explain the measurement have been put forward, and those which best explain the result require a follow-up experiment which probes the neutral weak couplings specifically using neutrinos. The proposed measurement is also interesting as an additional precision study at $Q^2 = 4 \times 10^6$ GeV^2. The two existing low Q^2 measurements are from atomic parity violation [3], and Moller scattering [4]. A careful, controlled

measurement of neutrino-elastic scattering should provide a measurement of the weak mixing angle at the level of 1%.

The technique of using reactor neutrinos to measure the weak mixing angle measurement has been pioneered by Reines, Gurr, and Sobel [5]. The weak mixing angle measurement comes mainly from tagging electrons that possess an energy greater than 3 MeV. Above this energy threshold, many of the environmental backgrounds are reduced or removed entirely. In order to make a precision measurement, the incoming neutrino flux has to be known to better than 0.5%. Current uncertainties in nuclear fuel burning limit one's knowledge of the neutrino flux and spectrum to no better than 2%. Thus, it is necessary to use inverse beta decay events ($\bar{\nu}_e + p \rightarrow e^+ n$) as a normalization constraint. These events can be tagged by the subsequent neutron capture on Gadolinium. The inverse beta decay cross-section for low energy neutrinos is given by the following expression:

$$\sigma(E_{e+}) = \frac{2\pi^2}{m_e^5 f \tau_n} p_{e+} E_{e+} \tag{3}$$

Here, $E_{e+}(p_{e+})$ is the energy (momentum) of the outgoing positron, f is the free neutron decay-space factor, and t_n is the neutron lifetime. The total uncertainty on the cross-section is 0.2%, making it an ideal process by which to normalize electron scattering events.

To reduce the uncertainties associated with neutrino electron scattering, careful control must be placed on the backgrounds and systematics associated with counting the number of electrons and their subsequent recoil energies. Further details regarding background rejection and error reduction techniques can be found in Reference [6]. A total uncertainty of 1.3% is, in principle, achievable with sufficient flux, adequate overburden, and a careful calibration program. We believe such a measurement will greatly complement a θ_{13} measurement program at reactor experiments.

In addition to being a direct probe to the weak mixing angle, neutrino-electron scattering is also sensitive to other exotic physics. More notably, the differential cross-section $\bar{\nu}_e + e^- \rightarrow \bar{\nu}_e + e^-$ depends also on the neutrino magnetic moment, μ_ν. The Standard Model prediction for the neutrino magnetic moment is very small, $\mu_\nu \sim 10^{-19}\mu_B$. Thus, a positive measurement of μ_ν beyond this prediction would be a strong indication of new physics. The current limit from reactor experiments on the neutrino magnetic moment is less than $1.3 \times 10^{-10}\mu_B$ at the 90% confidence level [7]. Reactor experiments may be able to probe at this level of sensitivity or greater.

2 Strategy to reach sensitivity of $\sin^2 2\theta_{13} = 0.01$ in reactor experiment

2.1 Overview of Braidwood Experiment

2.2 Backgrounds

2.2.1 Overview

The ~ 30 μs coincidence between e^+ annihilation and n capture on Gd provided by the $\bar{\nu}_e p \rightarrow e^+ n$ signal reduces all serious background sources to a neutron capture on Gd in association with an uncorrelated or a correlated in-time energy deposition from another neutron or a radioactive decay in the detector. The correlated background has long been recognized as the most important. It arises almost entirely from cosmic ray muon spallation that creates the radionuclides ^{9}Li and ^{8}He inside the detector, and from spallation events in the experimental enclosure walls or shielding system that produce fast neutrons which then enter the detector. ^{9}Li/^{8}He each produce a neutron in their beta decays that mimics the antineutrino signature closely. Their 100-200 ms half-lives mean that it is difficult to veto these events by using a simple muon track coincidence without introducing prohibitive dead time. Fast spallation neutrons can enter the signal

sample through a sequence of hard elastic scatters with protons in the detector that produce 1-8 MeV of visible energy, mimicking a positron signal, that is then followed by the capture of the neutron through thermalization. Spallation neutrons also dominate the uncorrelated backgrounds, which occur when a neutron capture by chance takes place in coincidence with an energy deposition in the detector initiated by radioactive decay or by an independent spallation event.

These neutron-driven background rates may be theoretically uncertain to $\delta B/B \sim 50\%$ for fast spallation neutron production, and perhaps a factor of 3 for radionuclide production. This places high demands on the signal-to-background ration, perhaps $S/B \sim 100$ in each Braidwood detector after event selection cuts, in order to achieve an overall 1% sensitivity on $\sin^2 2\theta_{13}$, and, at the same time, calls for a designed-in capability to measure backgrounds in place. Despite these challenges, extrapolations from previous experiments and other studies indicate that these requirements can be met, provided that the detectors are at sufficient depth, that an effective active and passive shielding scheme is implemented, that radioactive impurity levels are kept under control, and that a robust triggering and data acquisition system is implemented.

The $\sin^2\theta_W$ determination calls for measuring the rate for $\bar{\nu}_e e^- \rightarrow \bar{\nu}_e e^-$ production without benefit of the positron-neutron capture coincidence. Requirements for the rejection and monitoring of spallation backgrounds are at least as high as for the $\sin^2 2\theta_{13}$ extraction; and substantially more stringent requirements on radioactive impurity levels must be imposed. The weak mixing angle measurement also necessitates development of more aggressive analysis strategies than for $\sin^2 2\theta_{13}$ that employ tight visible energy and reconstructed event vertex cuts. These issues are discussed elsewhere in this document.

The remainder of this section provides more details on background rate calculations; suppression strategies for fast neutrons, cosmogenic radionuclide sources, and intrinsic radioactivity; and in situ background measurement techniques.

2.2.2 Muon Flux and Neutron Production

All estimations of cosmogenic backgrounds require an accurate characterization of the muon flux at the detector. This mandates development of a good Monte Carlo generator tuned to external data and to the local geology as determined from bore hole samples (which are currently being obtained at the Braidwood site). Preliminary calculations[8] that employ a muon flux at the surface tuned to data and using GEANT4 to propagate the muons through a flat "standard rock" ($A = 22$, $Z = 11$, $\rho = 2.65$ g/cm^3) overburden appropriate for Braidwood yield flux and rate values for muons given in Table 1. The values are consistent at the 15% level with computations with the MUSIC[9] package that employ the Gaisser parameterization[10], and with determinations by CHOOZ[11] for similar depths.

Neutrons generated 50-200 GeV muons, the energy range where the muon flux peaks, arise from several processes of comparable importance, including direct muo-spallation, nuclear photodisintegration, and spallation by secondary pions and neutrons from muon-nucleus induced hadronic showers. Inclusive production rates are estimated by convoluting cosmic ray muon spectra with neutron muo-production formulae provided by Wang et al[12].

Of particular interest are the long-lived μ+^{12}C,^{13}C spallation products ^{9}Li$\big(Q = 13.6$ MeV, $\tau_{1/2} = 178$ ms$\big)$ and ^{8}He$\big(Q = 10.7$ MeV, $\tau_{1/2} = 119$ ms$\big)$, with 49.5% and 16.1% branching fraction $\beta + n$ decay modes, respectively. The correlated electron ionization/neutron capture signature from these radionuclides can easily mimic the $\bar{\nu}_e p \rightarrow e^+ n$ signal. Furthermore, the decays occur so long after the passage of the initiating muon track that simple veto schemes are ineffective in removing them from the signal sample. Production estimates for ^{9}Li/^{8}He are obtained by assuming that the ratio of radiocuclide to inclusive spallation neutron is the same as in KAMLAND[13]. The radionuclides ^{12}B $\big(Q = 13.4$ MeV, $\tau_{1/2} = 20.2$ ms$\big)$ and ^{12}N $\big(Q = 17.3$ MeV, $\tau_{1/2} = 178$ ms$\big)$ production rates are given as well since they provide spallation rate monitors and serve as useful calibration sources; their rates are estimated by the same procedure. Horton-Smith has argued[14] that this technique overestimates radionuclide production rates at shallow sites (in particular, Chooz) by a factor of $4-5$ because the bulk of the production at KAMLAND is due to hard secondary neutrons spallating nuclei in the detector; and the production rate for these energetic secondaries

Quantity	D=300 mwe	D=450 mwe
$\bar{\nu}_e$ interaction rate– near detector	55 day^{-1}ton^{-1}	55 day^{-1}ton^{-1}
$\bar{\nu}_e$ interaction rate– far detector	1.8 day^{-1}ton^{-1}	1.8 day^{-1}ton^{-1}
mean muon energy	61 GeV	83 GeV
muon flux	0.46 m^{-2}s^{-1}	0.16 m^{-2}s^{-1}
6.5 m detector muon rate	15 Hz	5.4 Hz
inclusive neutron production rate	303 day^{-1}ton^{-1}	138 day^{-1}ton^{-1}
6.5 m detector neutron rate	0.39 Hz	0.18 Hz
^{12}B/^{12}N production per day	8.0 day^{-1}ton^{-1}	3.7 day^{-1}ton^{-1}
^{8}He/^{9}Li production per day	0.034-0.15 day^{-1}ton^{-1}	0.016-0.07 day^{-1}ton^{-1}

Table 1: Muon and cosmogenic neutron properties expected at two candidate Braidwood depths. Muon rates and energies are from Ref. 8. Inclusive neutron rates are obtained by convolving these muon rates with production spectra from Ref. 12. The upper numbers for radionuclide rates are obtained by assuming the same excluse/inclusive production ratios at KAMLAND as obtained from Ref. 13. The lower rates are from Horton-Smith's model described in Ref. 14.

decreases more rapidly with energy than the inclusive neutron rate in scaling to the softer cosmic ray spectra of Braidwood or Chooz.

2.2.3 Fast Neutron Shielding

Fast neutron correlated backgrounds can be reduced by combination of active and passive shielding that surrounds the detector. Active shielding in the form of scintillation counters or wire chambers, provides a muon veto and muon tracking information for use in offline analysis. The ~ 1 mwe of passive shielding between the active shield and that detector and the ~ 90 cm thick outer buffer layer of mineral oil inside the detector attenuates the flux of spallation neutrons reaching the detector from the surrounding rock. Several R&D tasks must be carried out to optimize the shielding, including: (1) establishing the required size and coverage of the active shield; (2) establishing whether the passive shielding needs to provide 4π coverage; (3) establishing whether the active shielding must extend beyond the enclosure walls, especially along the top; (4) establishing the required veto efficiency of the active shield; (5) establishing the tracking resolution needed for the active shield; (6) choosing the best technology choice for the active shield; and (7) determining how the shielding is to be installed and supported– especially the ~ 100 tons above the detector and the ~ 100 tons that will need to be moved in place between the detector and the surface shaft once the detector is installed.

2.2.4 Suppressing Cosmogenic Radionuclides

Backgrounds from spallation-produced radionuclides produced inside the detector are harder to eliminate due to the long half-lives of ^{9}Li and ^{8}He and the nearly identical detector response of these correlated $\beta - n$ decay pairs to the $e^{+}n$ antineutrino production signal. Fortunately, measurements at CHOOZ[11] and KAMLAND[13] indicate that ^{9}Li/^{8}He cross sections are tolerably small ($S/B \gtrsim 10$ with no cuts); and there are some prospects for improving the precision of these measurements on the short term at KAMLAND. It would be valuable, however, to obtain further constraints on these and other radionuclide production rates at depths more similar to Braidwood's at something like the VSPLAT facility.

Possible extra handles[13] that might be available using the data itself include: (1) an ability to remove events off-line in which the positron-like primary ionization signal is spatially correlated with the track position of a muon passing through the detector within a specified time window before the event of interest, and (2) an ability to remove events offline in which the neutron capture is correlated with a muon-induced shower detected either in the detector or the veto system. Implementing the former procedure requires

study of the muon tracking resolution, the neutrino detector vertexing resolution, the optimal time window, and the data acquisition scheme. Implementing the latter requires similar studies plus development of a procedures to identify a muon-induced shower using the veto system either alone or with the neutrino detector.

In principle, it is possible to discriminate via pulse shape analysis neutron-generated proton recoils from the ionization/annihilation signal from $\bar{\nu}_e$-induced positrons, although this technique has enjoyed limited use to date. Implementing this scheme in Braidwood would require an R&D program in fast neutron and recoil proton response in the scintillator. oil, and a method to monitor and calibrate the technique during actual data taking.

2.2.5 Controlling Intrinsic Radioactivity

Beta and gammas from U, Th, and K decay chain products in the PMT glass, scintillator., support structures, and atmosphere can produce ≥ 1 MeV energy depositions in the detector that can form an accidental coincidence with a stray neutron produced by neutron spallation in the external rocks. For the $\sin^2 2\theta_{13}$ measurement, procedures must be developed to limit U/Th levels to $\sim 10^{-12}\,(10^{-10})$ g/g concentrations in the scintillator(acrylic); the tolerances for K are two orders of magnitude looser. These levels are well above those achieved by KAMLAND, BOREXINO, and SNO (although these experiments do not use Gd-doped scintillator.); and they have been achieved in the past by the Palo Verde and Chooz experiments. A procedure must be developed to insure that the Gd does not carry contaminants into the system; this will likely require a method for cleaning the scintillator. and Gd separately before making the final mixture, as was done in Palo Verde and Chooz. Assuming these levels can be achieved in the scintillator and acrylic, then the singles rate is expected to be dominated by PMT radioactivity, where K(U/Th) levels of 60 ppm(30 ppb) can be achieved using low radioactivity glass. The critical detector parameter for determining the singles rate from radioactivity is the thickness of the outer mineral oil buffer. This must be studied carefully using Monte Carlo techniques both to optimize the overall experimental S/B (a thinner buffer means more signal and more background), and to account for the complicated PMT geometry at the outer wall, the mineral oil-acrylic wall interface, and other non-trivial material and geometric effects

2.2.6 *In Situ* Monitors

Background rates *must* be measured; and it is therefor imperative to design the triggering and data acquisition system to tag and record as many of the important types of these interactions as possible. For both types of spallation backgrounds this can be accomplished by ensuring that the data acquisition system is capable of tagging muon tracks in coincidence with a delayed neutron signature. Issues to decide include the aforementioned required tracking resolution of the veto system and the specific triggering schemes. Extending the area of the active veto beyond the size of the enclosure roof would permit better studies of fast neutron production in the surrounding rock.

Uncorrelated background rates can be measured in the data by examining neutrino candidate events in which the neutron-like energy signal comes in at many capture time constants after the positron-like signal, or by selecting events using the "swap" technique[15], wherein the positron selection criteria are interchanged with the neutron selection criteria. An ability to tag the 164(0.3) μs time correlated ^{214}Bi-^{214}Po(^{212}Bi-^{212}Po) $\beta\alpha$ decays from the ^{238}U(^{232}Th) chain will allow constraints to be placed contributions from radioactivity in the oil and acrylic.

2.3 Calibration

For a two-detector reactor experiment, we need only understand the differences in acceptance between the two, and not the absolute detection efficiency. The detection efficiency ultimately depends upon what cuts we choose in our final analysis, but we will assume here only cuts on the positron and neutron energies and

the coincidence time between the two detectors. The difference in overall detection efficiency between the two detectors then depends primarily on a small number of response parameters:

1. The number of hydrogen targets
2. The Gd loading fraction
3. Scintillator light output, including aging effects
4. Detector optics, including the attenuation lengths of the different media (five for a three-zone detector, three for two-zone), PMT angular and wavelength response, Rayleigh scattering, and diffuse and specular reflection off of all media
5. Number of working PMT's, as well as their individual gains and efficiencies
6. Number of working electronics channels and individual efficiencies
7. The livetime of each of the two detectors

All of these items may change with time, and furthermore can create position dependences within the detector which in turn may depend on time. The parameters can be measured individually and then used in the context of a detector model (such as a Monte Carlo simulation) to predict the relative detector efficiencies, or they can be measured in an integral way by using a source identical or nearly so to the antineutrino signal. In practice, we expect that we will use both approaches, and in so doing not only be able to calibrate the two detector efficiencies relative to one another but determine the systematic uncertainty on the calibration.

The primary goals of the calibration program are therefore:

- To measure differences in the two integral detector responses directly through radioactive source deployments, *in situ* calibrations (spallation products and neutrons from reactor antineutrinos), and possibly detector movement
- To measure the individual response parameters in order to build detector models for use in the efficiency calibration and the determination of the relative systematic uncertainties between the detectors
- To provide an analytic form of the detector response so that each event's measured PMT hits, charges, and times can be re-mapped into event energy [1]

For the first goal, we will need to be able to deploy various radioactive sources at many positions within the volume of both detectors (using the same physical source for each detector). We also need to be able to accurately tag cosmic-ray spallation products, so that they can be used as calibrations and checks which can illuminate the entire active detector volume.

For the second and third goals, we will need to deploy optical sources of various wavelengths both inside and outside the active volume, at as many points as are necessary to measure the bulk optical properties of all the detector media. We will also need to develop a full detector model which includes the light generation (both scintillation and Cerenkov light), propagation (using the measured optical parameters), and detection.

2.4 Proposed Work

Well before the design of the detectors and calibration systems, several basic questions need to be answered: How many positions within the detector volume will sources need to be deployed? How well does the angular and wavelength distribution of optical sources need to be known—and how well can they be known in a low-cost, practical system? How well must the source position be known to calibrate the position-dependence

[1] We note that with a two-detector experiment, such an explicit reconstruction of event energy is not strictly necessary. The differential response function for the two detectors can be cast to map neutrino energy into observed hits and charges, rather than into observed energy, removing the energy calibration step.

of the response functions? Can there be differences between the detectors which are not seen by *in situ* calibrations like the inverse β-decay neutron capture peaks, and cosmic-ray spallation nuclei? How well matched do radioactive sources need to be to the expected signal and backgrounds, in order to be useful?

Much of the work to answer these questions will necessarily be done by simulation. For such a simulation to be useful, it must be based upon input parameters taken from measurements of the actual detector media. We would therefore like to being a research program whose goal is the measurement of many of these properties, and we list the many of the most important of these below.

2.4.1 Photomultiplier Tubes

Based upon the experience from detectors like the Sudbury Neutrino Observatory, we believe that a large part of the point-to-point variations in response will be due the response of the PMT's to light at different angles. For events occurring near the edge of the active volume, the near-side PMT photocathodes will on average be illuminated by high incidence angle photons. For events nearer the center, the photons tend toward normal incidence. The position sampling we will use for source calibrations will therefore depend on how steep the PMT response is with incidence angle, and this response is something we must measure now.

In addition to angular response, to build a complete model we will need to measure the charge and timing spectra (including any late- and pre-pulsing) for the various PMT's we may consider using in a complete experiment. Stability issues—such as the gain variation as a function of high voltage setting or PMT age, the PMT noise rates as function of temperature, light illumination, and age, and possible failure modes all need to be investigated and measured.

2.4.2 Scintillator

The model we use to predict the source response within the detector (which will be used to determine which sources are needed for calibration and what we can learn from them) depends directly upon the distribution of scintillation photons as a function of particle energy and species. We therefore need a measurement of the scintillator photon creation as soon possible.

The attenuation length, scattering length, and index of refraction all need to be measured and optimized for a full detector.

If the scintillator can change either in its optical or light creation properties, the two detectors may evolve separately. We therefore need to begin studies of how much the scintillator does change, in what ways it changes, and how predictable the changes are.

The scintillator timing for various mixtures also needs to be measured and input to the simulation, to determine how well the position of events can be reconstructed.

The neutron capture efficiency as a function of the Gd loading will also be critical for the simulation model, and will help to tell us how well we need to measure the capture efficiency between the detectors and the time dependence (if any) of that efficiency.

In addition, we will need to develop of a directly way of measuring the source strength of our neutron source (either an Americium-Beryllium source and/or a ^{252}Cf source) to much better than 1%, so that the relative capture efficiency between the two detectors can be measured and checked.

2.4.3 Acrylic and Oil

The same optical properties which need to be measured for the scintillator will need to be measured for the remaining media in the detector. For a 3-zone detector, the unloaded scintillator will also have to be measured.

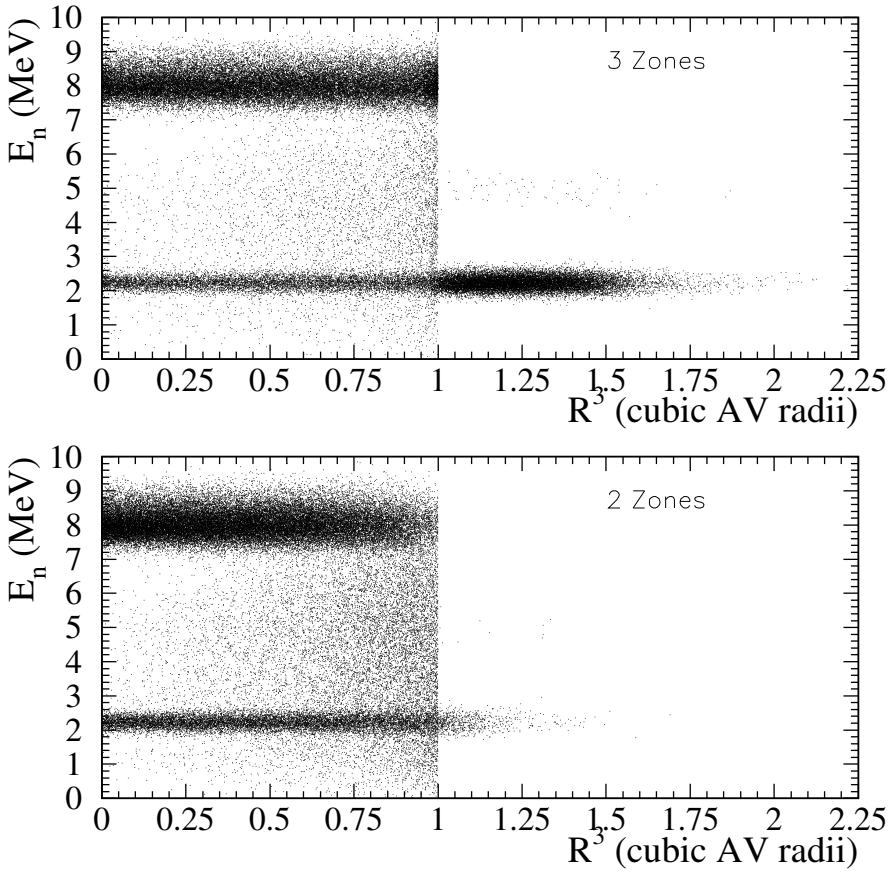

Figure 3: Simulated energy of neutron capture events vs. R^3, where $R^3 = 1$ is the radius of the inner scintillation volume.

2.5 Two-Zones vs. Three-Zones

We have adopted in this proposal a 'baseline design' which has two inner zones: an active Gd loaded scintillator volume, and an outer mineral oil volume. Although we believe that in a two detector experiment a two-zone design is superior to the three-zone designs discussed by other groups [**?**], part of our work under this proposal will be to determine both the efficacy of the two-zone design and the relative cost implications of two- and three-zone designs.

The motivations for a three-zone detector seem on the face of it to be excellent: the middle volume filled only with scintillator 'flattens out' the radial dependence of the energy response to neutrons. Figure 3 illustrates the basic idea. The top panel of the figure shows the energy response for neutron captures as a function of the volume-weighted radius $R_V^3 = (R/R_{\rm av})^3$ in a two-zone detector. The 8 MeV Gd capture peak and the 2.2 MeV H capture peak are clearly visible. There is also a 'wash' of events falling away from the Gd peak which becomes more populated as R_V^3 gets closer to 1.0. By contrast, the bottom panel of Figure 3 shows the response for a three-zone detector, and we see that the entire tail on the Gd capture peak is confined to a very narrow region near $R_V^3 = 1.0$. The basic point is well-known: the middle scintillation region of the three-zone detector 'catches' the neutron-capture γ rays which otherwise would leak into the mineral oil buffer and produce relatively minimal Cerenkov light.

Understanding the neutron response in the two-zone detector is therefore in principle more difficult—small changes in the detector's optical and energy response can lead to relatively large changes in the number of detected neutrons, as the tail moves above and below the analysis threshold for neutron detection. We might therefore expect that the calibration requirements for a 1% disappearance measurement are more

manageable in a three-zone detector.

The second motivation for a three-zone detector is that events created near the edge of the loaded volume can produce positrons which leave and annihilate outside. In a two-zone detector, the annihilation γ's for such positrons can produce at most a single γ which interacts in the scintillation region, thus the annihilation 'edge' at 1 MeV in the positron spectrum is broken, and the positrons can leak down to zero energy. In a three-zone detector, these events only occur at the edge of the middle region, and are thus eliminated simply by requiring the neutron energy to be consistent with Gd capture.

The third motivation for a three-zone detector is that the middle scintillation region provides an additional way of tagging fast neutrons. A large fraction of these will produce a recoil proton in the middle scintillation region before entering the inner loaded scintillation volume. These events can then be cut by the tag from the middle region, even if they produce a time-correlated event pair in the inner region.

All of these motivations are well-grounded, but become far less compelling in a two-detector experiment in which only *relative* response uncertainties matter. For example, an understanding of the neutron response can be made using the neutrons themselves—the neutron peak is narrow enough that it provides an excellent measure of the overall detector response. Most importantly, unlike any potential calibration source, the neutrons integrate over the detector volume and livetime in exactly the way we need. In our simulations, we have found that matching the neutron peaks between the near and far detectors reduces even huge (10%) differences in the energy scale between the two detectors, and we are investigating whether we can also use the overall shape of the neutron peak to investigate potential scale non-linearities.

Our simulations have also shown us that the total positron leakage below the annihilation edge in a two-zone detector is a few percent or less (and of course gets smaller with a large fiducial volume), and depends almost entirely on geometry. We expect therefore to know this already small fraction very well.

The middle region in a three-zone detector which tags the external neutrons can be effectively replaced in a two-zone detector just by a larger fiducial volume. The events which would have produced recoil protons in the middle volume followed by a coincidence pair in the inner volume will now produce a triple and therefore be tagged in a two-zone detector just as effectively.

The three-zone detector also has many drawbacks. In addition to the obvious construction difficulties, the three-zone detector introduces two new optical media (the scintillator and its container) which will need to be calibrated in order to understand the response to the neutrino signal and backgrounds (there is no neutron signal which can be used in the middle volume). The optical calibrations cannot be done by sources only in the mineral oil buffer and the inner volume—there is no way to untangle the covariances in the attenuation lengths. Sources will have to be deployed in the middle volume, and how this could be done (and with what cost in mechanical apparatus) would have to be explored. The new media will also attenuate the light somewhat, reducing the energy resolution and making it somewhat harder to see the positron annihilation edge or to separate signal from background. Lastly, the addition of a container for the middle volume also has the danger of adding backgrounds and increasing the accidental rate.

2.6 Cross Checks

The relative normalization of the near and far detectors is sensitive to several parameters: the target hydrogen density, the target volume, the detector efficiency, and the energy scale calibration through analysis cuts. In-situ calibration systems will play a large roll in understanding the efficiency and energy scale, but the hydrogen density and target volume cannot be determined in this way. The Double-CHOOZ collaboration [**?**] has proposed using various control and measurement procedures during detector assembly to ensure that the target vessels and target chemestry are identical, but even in their best case scenario they are only able to get the uncertainty on the relative normalization down to 0.6%. While we intend to implementing similar procedures during assembly, the Double-CHOOZ plan does not provide a way to verify that the assumed precision of these methods is correct. The plan for Braidwood is to construct movable detectors which will allow an independent, high precision measurement of the relative detector normalization.

2.6.1 Moving Detectors

The reactor neutrino flux itself provides one of the best means of determine the relative normalization of near and far detectors. The neutrino interactions sample the detector volume uniformly, and the energy, spatial and temporal characteristics of the events are, by definition, exactly matched to the events under study. The trick is to use the near detector site, where the interaction rate, or flux, is 30 times larger than at the far site. By placing two detectors side-by-side in the near detector hall where both detectors experience the same flux, one can determine their relative normalization ($\equiv \frac{N_1}{N_2}$), at that moment in time, with the statistical precision determined by the number of events observed:

$$\sigma_{relative} = \sqrt{\frac{1}{N_1} + \frac{1}{N_2}} \approx \sqrt{\frac{2}{N}} \tag{4}$$

where N_1 and N_2, the number of events observed in detectors 1 and 2, are approximately equal ($N_1 \approx N_2 \equiv N$), as would be expected for identical detectors. Given the Braidwood neutrino flux, the baseline detector size and near site location, an uncertainty of 0.25% could be achived in fewer than 100 days of side-by-side calibration running (less than 10% of the proposed experimental run).

Using this direct measurement of the relative normalization in conjunction with concurrent measurements of the detector efficeincy and energy scale, one can determine the target volume and hydrogen content. If the target temperature is maintained at a consistant value, the hydrogen content and target volume should be constants. Therefore these measurement values can be used to determine the relative normalization to high presision even when the far detector is located in the far position.

If during the course of the expreiment the detector efficieny can be shown to be stable and the analysis, which is insensitive to any fluxtuations in the energy scale calibration, can be defined then the uncertainty in relative normalization will reach the lower limit set by the side-by-side calibration. This hypothesis could be firmly established by comparing side-by-side calibrations runs taken early in the experimental run to thoes taken at the end.

2.6.2 Multiple Detectors

The requirement of movable detectors puts limits on the detector size and weight. These limits are set by shaft and tunnel appatures, and by the capacity of the crane or other lifting system. Multiple detectors allow one to achive the desired target mass within the constraints set by a practical and cost effective facility design. In the Braidwood experimental baseline, two far detectors are assumed. Each detector is 7 meters in diameter and weights about 165 metric tons. The correponding target mass is 65 tons per detector or 130 tons total target mass. The baseline also calls for tow near detectors. The use of multiple near detectors is motivated by the potential to measure the weak mixing angle.

Multiple-movable detectors allow for greater flexibility in operating the experiment. For example, if it turns out that $\sin^2 2\theta_{13}$ is very small, then it is possible to redeploy the second near detector as a far detector (or to build additional far detectors) to increase sensitivity to the spectral shape distortion [**?**].

If the relative normalization uncertainties between n far detectors are uncorrelated then when the results of the different detectors are combined the effective relative normalization is reduced by $\frac{1}{\sqrt{n}}$. The condition of uncorrelated uncertainties is satisfied if the method of determing the uncertainty comes from independant measurements such as separate side-by-side calibrations.

2.7 Questions and proposed R&D

3 Proposed Engineering for Cost and Schedule Determination

3.1 Proposed engineering for Cost and Schedule Determination

3.1.1 The Braidwood Site

The Braidwood Nuclear Station is located about 90 km southwest of Chicago. The plant is built next to an old coal strip mine which has been converted into a cooling lake. The terrain at Braidwood is very flat with a change in elevation of less than two meters over the region of interest. The plant consists of two reactors each with a rated maximum thermal energy of 3586 MW. Averaged over the last eight years both reactors have operated with a capacity factor of greater than 90% and capacity factor has continually improved throughout this period. The two reactors are separated by about 100 meters running north-south (see Figure 4). The reactors sit in the middle of a rectangular security area. All experimental facilities must be located outside this security fence. Outside the fence, the point of closest approach is on the east side at a distance of about 200 meters from the reactors.

To get the required cosmic ray shielding the detectors will be located at the bottom of two shafts, one at the near site and one at the far site. (Figure 5 shows the proposed layout of the facility.) The shafts will be dug to a depth of 115 to 170 meters (300 to 450 meters water equivalent (mwe)). Geological data collected during the planning and construction of the plant [17] show a rock formation, known as the Galena/Platteville, that begins at a depth of about 85 meters and extends to nearly 200 meters. The Galena/Platteville formation is made up of dolomitic limestone, a rock type that is typically good at supporting tunnel structures. In addition, the radioactivity of limestone is typically low compared to most other rock types. The low intrinsic radioactivity of this specific rock group is confirmed by several gamma surveys performed during the original site characterization studies [17]. It is in this layer that the detector rooms will be constructed. The actual depth will be determined by the results of a core boring study that is currently in progress. The rock cores and bore holes will provide data on rock strength and water flow rates which will be used to determine the

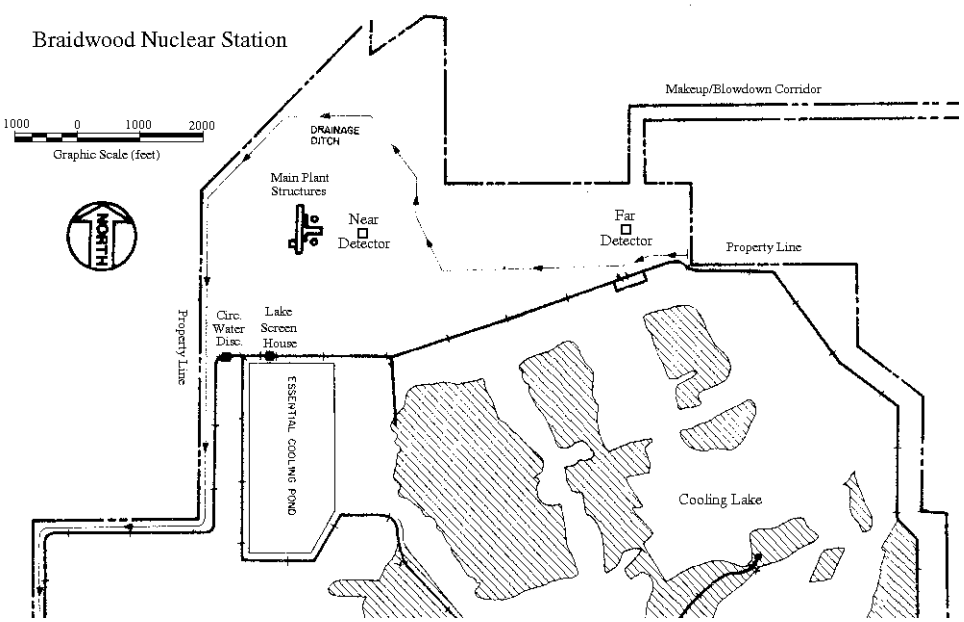

Figure 4: Drawing of the plant and surrounding area showing the approximate locations of the near and far detectors with respect to the plant and cooling lake.

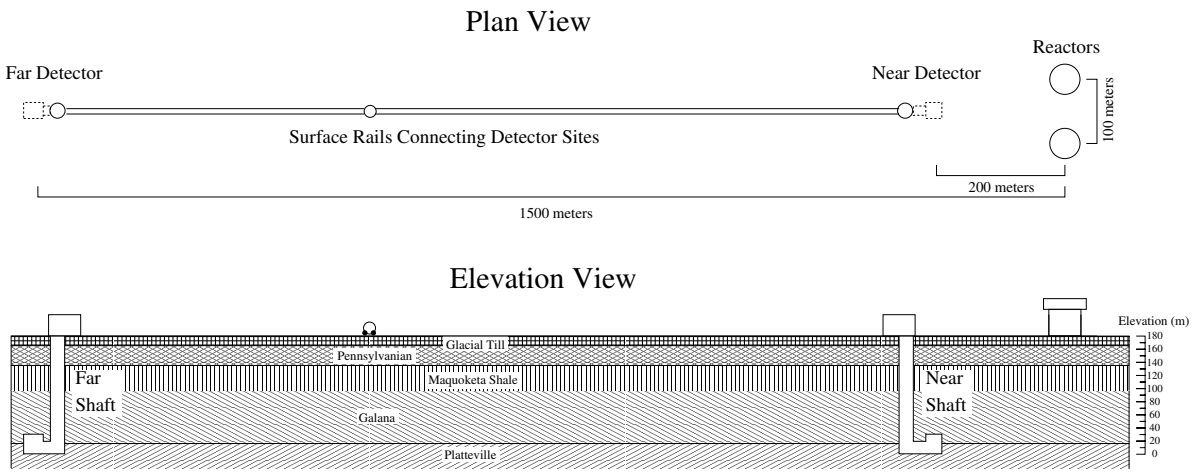

Figure 5: Plan and elevation views of the proposed layout of the experimental facility are shown. The elevation view shows the the major geological strata and their approximate elevation, in meters above sea level. Buildings, shafts and detectors are not drawn to scale.

feasibility and cost of civil construction and maintenance as a function of depth. From a physics point of view, deeper shafts are preferable since background rates and dead time decrease with depth. On the other had, depth may be a cost driver for the experiment and it may not make sense to go below where background uncertainties are the limiting systematic. Continuing this cost benefit analysis will be a high priority in the coming year.

3.1.2 Baseline Design

In the baseline design the detectors halls are located due east of the reactors on the line that is equidistant from both reactors. The near detector hall is just outside the security fence (∼200 meters) and located 175 meters (450 mwe) below the surface. Therefore the neutrino path length distance is approximately 270 meters. The far detector hall is 1500 meters due east of the reactors and is also down 175 meters which results in a neutrino path length of about 1510 meters. The baseline calls for two detectors at each site, each with an outer diameter of 7 meters. Each detector will be surrounded on 5 sides by a veto system that has an array of active cosmic ray detectors outside about a meter of passive shielding. Each detector sits inside a veto which is housed in an excavated room of dimensions 12 meters wide, 11 meters high and 32 meters long. Each room holds two complete detector-veto systems.

Ten meter diameter shafts connect the surface to the detector level at both the near and far sites. Each shafts contains two elevators, ventilation ducts, electrical and data cables, as well as pumps and water pipes for removing water from the shaft sump. The detector halls are connected to the shaft by a tunnel stub. At the far end this stub will be approximately 10 meters in length, which is the minimum required for structural integrity. The near tunnel stub will be about 45 meters long, because surface infrastructure at the near site does not allow construction of the shaft directly above the detector hall location.

In March of 2004, the collaboration commissioned a study of the cost and schedule of constructing an underground neutrino facility at the Braidwood site. The study was conducted by the consulting firm of Don Hilton and Associates. The results of the study were presented in such a way that cost of specific tasks could be broken out into manageable units (cost/meter of shaft, of tunnel, etc.) and rearranged to optimize the physics potential per unit cost. Table 2 show the estimated cost of the baseline civil construction as determined using the results of the Hilton study. The 17% scale factor for EDIA (Engineering, Design, Inspection and Administration) is consistent with industry standards for a project conducted under a design and build contract [18]. The 25% contingency assumes that the rock conditions along the full length of each

Description of Work	Quantity	Units	Unit Cost	Subtotal	Total
General Mobilization	1	each	$3,286,691	$3,286,691	$3,286,691
Shaft					
mobilization	1	each	$512,165	$512,165	
pregrout overburden	15	meters	$7,538	$113,074	
excavate & line soil	15	meters	$62,891	$943,360	
excavate & line rock	160	meters	$42,262	$6,761,941	
water ring	1	each	$87,445	$87,445	
surface facilities	1	each	$104,532	$104,532	
equipment	1	each	$664,844	$664,844	
sump room	1	each	$226,295	$226,295	
decommissioning	1	each	$412,289	$412,289	
Shaft Total	2	each	$9,825,945	$19,602,870	$19,602,870
Detector Room (each room houses 2 detectors)					
excavate	32	meters	$69,156	$2,212,981	
grout	32	meters	$5,641	$180,511	
Detector Room Total	2	each	$2,393,492	$4,786,984	$4,786,984
Tunnel					
excavation	55	meters	$28,237	$1,553,035	
grout	55	meters	$2,247	$123,585	
Tunnel Total	55	meters	$30,484	$1,676,620	$1,676,620
Subtotal					$29,353,165
EDIA	17	%			$4,990,038
Contingency	25	%			$8,585,801
Total					$42,929,004

Table 2:
The cost of civil construction for the baseline project estimated using the study of Don Hilton and Associates.

shaft have been fully characterized, which will be the case when the shaft core borings are completed this October. The Hilton study estimates that each shaft and detector hall will take about 18 months to complete, with about 3 months on each end to mobilize and demobilize. The work on the two shafts can either be done serially or in parallel, so the civil construction should take between 2 to 3 1/2 years to complete.

3.1.3 Civil Engineering Needed for a Proposal Design Report

Developing the Scope for a Design and Build Contract Package The current plan for civil construction is to use a design and build contract [19]. In a design and build situation the collaboration specifies the layout, requirements and baseline design and the final design is determined by the contractor. This allows contractors the freedom to select techniques that they are already familiar with or to use equipment that they already own. The contractors know best how to use local labor, methods and means most cost-effectively. This can potentially result in a faster and less expensive overall project. The design and build process requires that the collaboration focus, early on, on developing a well-defined set of requirements that gives bidding contractors the maximum design flexibility. This will be a major activity in the next year as the collaboration prepares a full proposal.

In order to determine the requirements a significant baseline design study is needed. This study will include geotechnical, civil, electrical, and mechanical engineering. It will provide a framework for estimating cost and schedule, and for creating a bid package suitable for completing a design and build contract. The

Task	Cost (×1000)
Geology/Geo-technical	\$75
Civil/Structural	\$50
Electrical	\$25
Mechanical	\$25
Drafting	\$75
Cost & Schedule	\$25
Other Costs	\$50
Management & Administration	\$75
Detector Moving Study	\$25
Contingency	\$100
Total	\$525

Table 3: This cost estimate is made in increments of \$25K where one unit of \$25K represents 1 senior engineer-month or 2 junior-engineer months.

specific elements of this study, and their approximate costs, are discussed in the following paragraphs and they are summarized in Table 3. The cost estimate of this study is done to a precision of \$25K where each unit of \$25K represents 1 senior engineer-month or 2 junior engineer-months.

Geological and geotechnical engineering tasks will include the characterization of the ground units (or strata), and the determination of the ground water table and ground permeabilities in the various units. Viable options for excavation methods, rock support systems and water control will be identified. These studies are expected to cost approximately \$75K.

Civil and structural engineers will determine the requirements for all surface work platforms and buildings. They will also determine all needed utility runs and access roads. Underground they will look at shaft lining and floor requirements. These studies have an anticipated cost of approximately \$50K.

Electrical engineering tasks include determining the specifications for power and communications: power distribution, transformers, lighting, grounding, safety systems such as fire detection, phone and internet. The estimated cost of these studies is \$25K.

The mechanical engineering studies will determine the requirements for heating, ventilation, and air conditioning (HVAC), fire protection, ground water pumping systems, and other utilities. The approximate spatial layout and routing of pipes and ducts will also be determined. The mechanical engineering cost is assumed to be \$25K.

All engineering studies will result in a reviewed outline of the determined specifications, and text for the related sections of the bid and contract documentation. In addition these engineering studies will generate the drawings required to bid the contract. These will include scale-approximate schematics of the layout of the surface buildings, shafts, tunnels, and chambers. Accurate scale drawings will be generated for the existing surface conditions; the spatial envelope of the minimum required excavations; and for the baselines of the electrical, mechanical and structural design. Drafting costs are expected to to be about \$75K.

In the course of these studies a methodology will be determined for estimating the cost and schedule. A risk analysis will be made to help in setting the appropriate contingency. These tasks have been allocated \$25K. In addition, \$50K has been allocated for "other costs." These costs include a land survey, evaluations of environmental safety and health requirements, and permitting.

Finally, \$75K is allocated to project management. These tasks will include coordinating with Exelon, the funding agencies and the institutions of the collaboration; conducting the engineering reviews; and contractor selection and pre-qualification.

Detector Moving Study The experiment baseline specifies movable detectors which allow for an important cross check of the relative normalization of the near and far detectors as discussed in Section 2.6.1. In

addition movable detectors allow the detectors to be built on the surface in a single facility, during the civil construction. Without this capability, the project would incur additional costs from installing clean rooms and overhead cranes in each detector room. Also, transferring scintillator and other potentially toxic materials underground would present a significant environmental and safety hazard. Finally, detector construction, commissioning and testing could be conducted on the surface, during civil construction so that the detectors are ready to be installed as soon as the halls are complete.

The issue of how best to lift a 150 to 200 ton detector from the bottom of a 175 meter deep shaft, move it across 1300 meters of flat land, and lower it down a second 175 meter shaft must be addressed in the full proposal. The Fermilab Facilities Engineering Services Section (FESS) is currently in discussion with the Belding Walbridge Company about the cost and scope of such a study. Belding Walbridge is a contractor in heavy lifting and rigging and has worked with Fermilab in the past.

This study will divide up into two phases. In the first phase Belding Walbridge will develop a small number of initial schemes including sketches and order of magnitude cost estimates. In the second phase the collaboration will select one of these schemes for further development. This development will include scaled drawings; a detailed cost estimate that separates one-time costs – such as equipment – and recurring cost for each move operation; and a move schedule detailing the time required for each detector move. The estimated cost of this study is $25K.

3.2 Detector R&D

3.2.1 Introduction

The Argonne group in the Braidwood collaboration is performing the detector engineering for A new experiment to be located at the Braidwood nuclear power plant to study electron antineutrino disappearance to measure of limit the important neutrino mixing parameter θ_{13}. The important features of the experiment design are to locate one 25 ton (fiducial volume) detector about 200 m from the average core position, and another two identical 25 ton detectors at a distance of about 1.5 km. Both detector sites need to be under sufficient overburden that muon induced spallation products do not produce a significant amount of correlated background, and are at the bottom of shafts with an overburden of at least 400 MWE.

A baseline design has been completed for the detector. However, detailed work needs to be completed on the detector structure and further R&D is needed on designing structures with acrylic and scintillator. This section outlines a plan for 2005-2006 to address remaining R&D questions/issues about the mechanical design in order to have a detector design that is ready to go out for construction.

3.2.2 Detector Design

Below is a list of tasks and estimated effort required to develop a complete detector design.

- *Design of Acrylic Sphere* Significant work has already been completed on the requirements for designing and constructing large acrylic sphere[20]. However, additional work is needed to investigate the method of bonding, develop a final design for supporting the structure, and perform a detailed structural analysis.
  - Engineer - 2 month FTE
  - EA - .5 month FTE
  - Designer - .5 month FTE
  - $4k M&S to perform bonding tests
- *Design of Outer Steel Sphere* The outer steel sphere is used as a containment vessel and must be constructed in two halves joined by a flange in order to provide access to the PMT's. Work is needed

design the basic sphere, design the flange connection, and to identify vendors who can construct such large spheres.

  - Engineer - 2 month FTE
  - Designer - .5 month FTE

- *Calculation of Pressure Variation Inside Detector* During the movement of the detector lateral accelerations will result in variations of the pressure distribution inside each sphere. Calculations are needed to determine this variation in order to see the maximum pressure that the PMTs will be subjected to and if a potential shock wave effect could occur because of very high accelerations. Also, the potential for damage due to a PMT exploding needs to be investigated.

  - Engineer - .5 month FTE

- *Development of Assembly Procedure* A procedure is needed for assembling the detector. This involves designing the fixtures, tools, and procedures for assembling the acrylic sphere inside the outer steel sphere, mounting the PMT tubes, and mounting the steel sphere inside its support structure

  - Engineer - .5 month FTE

- *Design of PMT Mounts* The method for mounting the PMT inside the steel sphere has to be developed.

  - Engineer - .25 month FTE
  - Designer - .25 month FTE

- *Design of Detector Support Structure* The structure that will support the detector and will be used for lowering into the cavern and for movement inside the cavern needs to be designed.

  - Engineer - 2 month FTE
  - Designer - .5 month FTE

- *Scintillator/Acrylic Investigation* The potential of scintillator crazing the acrylic needs to be investigated for the proposed makeup of scintillator.

  - Engineer - .5 month FTE
  - EA - 1 month FTE

- *Scintillator Handling/Storage and Detector Filling Procedure* The inner and outer spheres will be filled at the same time. This will require accurate control of the fluid flow rate. Also, it is required that the liquid in each detector be identical which can only be achieved if the liquid is mixed on site and the detectors filled at the same time. This will require large storage tanks on site and a piping system for mixing and filling.

  - Engineer - 1 month FTE
  - EA - 1 month FTE

- *Detector Transport System in the Cavern* The detector structure will rest on a set of Hillman rollers. The rail system and method of pushing/pulling the detector needs to be designed for moving the detector after it has been lowered into the cavern.

  - Engineer - 1 month FTE
  - Designer - .5 month FTE

- *Method for Moving Detector Between Far/Near Sites* The detectors will be moved relatively infrequently between the far and near sites. However, given the large size/weight of the detector it may be impractical to move them on by a truck. A dedicated rail line between the sites has to be designed and a simple way of moving the detectors along this rail must be developed.
  - Engineer - 2 month FTE
  - Designer - .5 month FTE
- *Above Ground Facilities at Near/Far Sites* The surface buildings/crane/office space at the near and far detector sites must be designed and costed.
  - EA - 2 month FTE
  - Designer - .5 month FTE

3.2.3 Total Effort

The total Argonne effort for developing a final mechanical design for the Braidwood Reactor experiment that is ready for construction is 11.75 FTEmonths for Engineering at $15,972 per FTEmo, 4.5 FTEmonths of Engineering Assistants at $15,972 per FTEmo, and 4.5 FTEmonths of Design work at $9,416/FTEmo. The total estimated expense, including $4,000 M&S is $353,000 as shown in Table 4

Item	Units	Unit Cost	Cost
Engineer Effort	11.75	$16,000	$188,000
EA Effort	4.5	$16,000	$ 72,000
Drafting	3.25	$9,400	$ 30,550
Materials and Supplies	n/a	n/a	$ 4,000
Contingency		20%	$ 58,900
Total			$353,000

Table 4: Estimate of Detector Engineering Costs for the Braidwood Reactor Neutrino Project

4 Outreach Possibilities

Three subject groups for outreach are considered. The first are people in the local area, the second are students, and the third is the population at large.

4.1 Local Area

A list of talk topics and speakers will be distributed to local organizations (Kiwanis,...) and schools. Some sample topics might be:

- What are the big physics questions today?
- Do we still need basic research?
- Nuclear engineering; Reactor monitoring and safety.
- General energy management
- Particle physics; what are we trying to measure and why?
- History of the neutrino

- Nuclear physics
- Astrophysics

The excitement of new discoveries will be emphasized. The present day discoveries are unifying the understanding of the very large (the universe) and the very small (sub-atomic forces and particles). Some of these things are understood (quarks, basic strong and electroweak forces), and some are not (dark matter and energy). Black holes, wormholes, extra dimensions and other wild, yet possible aspects of the real world will be discussed.

Many of the discoveries which changed the world and established the economic leadership of the USA during the twentieth century came from basic research. Nuclear power, lasers, superconductors, transistors, all came from basic research. The world-wide web came as a spinoff of particle physics basic research. Most of these discoveries were unanticipated in advance, even by the experts in the field. Targeted research would not have found them.

Reactor power will certainly have to be maintained and almost certainly expanded in the near future. Although some public concerns are justified, there is a fear factor for many people that is considerably worse than justified by the facts. Some discussion of the safety record of existing reactors (except in Russia) will be made. The role of this experiment in providing an independent monitor of the reactor flux could be described.

The fascinating phenomenon of neutrino oscillations can be discussed as well as the violation of fundamental symmetries. The role of the measurement of θ_{13} for the future of this line of research will be described as will some of the projected future experiments with superbeams and neutrino factories, utilizing detectors hundreds or thousands of miles away from the accelerators.

The proposers will work with the Exelon Corporation to establish an office of outreach for the θ_{13} experiment. Publicity releases will be sent to local papers, TV and radio stations describing the project and its progress. When justified, the releases will go to national media. Researchers will be made available for interviews. Local people will be utilized for construction where possible, and this, also, will be publicized. We will try to develop an on-site welcome center that provides inquiry-driven experiences in content areas in which materials developed for web-delivery are adapted for live engagements. The welcome center will be tied into tours of the power plant.

4.2 Students

A Summer jobs program for college and possibly high school students will be established. They will help with construction and testing of prototypes and the detector, with PMT testing, and with electronics construction and testing. Cooperation with the American Physical Society and the American Association of Physics Teachers will be established for development of online activities as well as workshops and seminars.

4.3 Population at Large

A web site will be produced which will contain the information described above for talks. θ_{13}-specific activities will be bound into ongoing outreach efforts at universities and national laboratories. The site will be linked to education databases. A 1-2 page brochure on the experiment will be produced concerning physics. technology, and local aspects of the experiment.

5 Summary

References

[1] D. Y. Bardin, S. M. Bilenky and B. Pontecorvo, Phys. Lett. B **32**, 68 (1970).

[2] G. P. Zeller *et al.*, Phys. Rev. Lett. **88**, 091802 (2002) [Erratum-ibid. **90**, 239902 (2003)]

[3] S. C. Bennett and Carl E. Wieman, Phys. Rev. Lett. **82**, 2484 (1999).

[4] P. L. Anthony *et al.* [SLAC E158 Collaboration], Phys. Rev. Lett. **92**, 181602 (2004)

[5] F. Reines, H. S. Gurr, and H. W. Sobel, Phys. Rev. Lett. **37**, 315 (1976).

[6] J. M. Conrad, J. M. Link and M. H. Shaevitz, arXiv:hep-ex/0403048.

[7] H. T. Wong, arXiv:hep-ex/0409003.

[8] M. Hurwitz and J. Pilcher, "Simulation of Cosmic Ray Muon Flux at Shallow Depths Underground", http://braidwood.uchicago.edu/text/Muon.pdf (July, 2004).

[9] V.A. Kudryavtsev, N.J.C. Spponer, J.E. McMillan, Nucl. Instrum. Meth. **A505**, 638 (2003).

[10] T.K. Gaisser, *Cosmic Rays and Particle Physics*, Cambridge University Press, 1990.

[11] M. Apollonio et al. (CHOOZ collaboration), Eur. Phys. J. **C27**, 331 (2003).

[12] Y.-F. Wang, *et al.* Phys. Rev. **D** 64, 013012 (2001).

[13] T. Araki, et al. (KAMLAND collaboration), hep-ex/0406035 (June, 2004).

[14] G. Horton-Smith, "Quashing Backgrounds", 2nd International Workshop on Future Reactor Neutrino Experiments, Oct. 10, 2003, Munich, Germany, www1.physik.tu-muenchen.de/lehrstuehle/T30d/events/reactor03/pages/transparencies/horton-smith.pdf.

[15] Y.-F. Wang, *et al.* Phys. Rev. **D** 62, 013012 (2000).

[16] J. M. Conrad, J. M. Link and M. H. Shaevitz, arXiv:hep-ex/0403048.

[17] Exelon Nuclear, *Byron & Braidwood Stations Updated Final Safety Analysis Report*, December 2002.

[18] Jack de la Vergne, *Hard Rock Miners' Handbook*, MaIntosh Engineering Inc., 2003.

[19] Gary S. Brierley and David J. Hatem, editors, *Design-Build Subsurface Projetcs*, Zeni House Books, 2002.

[20] http://gate.hep.anl.gov/vjg/Reactor-Baseline1.doc